JOURNAL OF AGRICULTURAL AND FOOD CHEMISTRY

J. Agric. Food Chem. **2008,** *56,* 11453–11457 **11453**

Phenolic Acid Nanoparticle Formation in Iron-Containing Aqueous Solutions

LARS NILSSON,*,† DAVID LÖF,§,# AND BJÖRN BERGENSTÅHL†

Divisions of Food Technology and Physical Chemistry 1, Lund University, Lund, Sweden

This paper presents results which show that the interaction between two phenolic acids, *p*-coumaric and caffeic acid, with iron results in the formation of meta-stable colloidal nano particles. The particles are characterized with dynamic light scattering and cryo-transmission electron microscopy. The results show that the nanoparticle formation is an important feature of phenolic acids which is likely to have a large impact on the behavior of these substances as well as their functionality as antioxidants.

KEYWORDS: Phenolic acids; caffeic acid; coumaric acid; antioxidants; iron chelation

INTRODUCTION

In recent years, polyphenols and phenolic acids have attracted an increasing amount of attention. These compounds have the ability to inhibit oxidative reactions by chelating potential pro-oxidative metal ions such as iron (*1*), by scavenging radicals formed as a result of oxidation (*2*), or by quenching reactive species such as the singlet oxygen (*3*). Phenolic acids such as caffeic acid (3,4-dihydroxycinnamic acid) and *p*-coumaric acid (3-hydroxycinnamic acid) occur in a wide range of plants and foods. The chemical structures of these two phenolic acids are shown in **Figure 1**. Whether phenolic acids are absorbed and metabolized from the diet has been the subject of much debate. However, at present it has been shown that these substances are absorbed in the intestine and thereby potentially providing systemic antioxidative effects in vivo. Absorption has been shown from a variety of foods that include wine, beer, apple cider, and coffee (*4*−*7*).

The ability of polyphenols and phenolic acids to act as antioxidants has been studied to quite some extent and still raises large interest, particularly as antioxidants in emulsions. One reason for the wealth of studies is the complex nature of the substances. They may, for instance, act as both anti- and pro-oxidants, depending on conditions (*8, 9*). Furthermore, their role and activity in vivo are not yet fully understood. The majority of studies available in the literature deal with the nutritional, biochemical, or chemical structure aspects of polyphenols and phenolic acids (*10, 11*), whereas few studies address the physicochemical properties (*12*).

In emulsions it has been observed that very thick surfactant layers reduce lipid oxidation in comparison to thinner layers (*13*) and that introduction of cationic charges may repel pro-oxidants and, hence, have a protective effect (*14*). The most general observation is that hydrophobic antioxidants seem to preferably stabilize water continuous emulsions, whereas hydrophilic antioxidants stabilize oil continuous systems, commonly referred to as the "polar paradox" (*15*). Systematic discussions have assumed a partitioning between the oil phase, the aqueous phase, and also possibly an interfacial pseudophase (*16*).

In a recent study we had difficulties in characterizing any affinity of typical polyphenols and phenolic acids to the interfacial layers. Instead, we observed irregular solution properties resulting in the formation of a nanoprecipitate (*9*). Thus, it seems clear that the solution properties are essential when the complex antioxidant properties of phenolic antioxidants are to be characterized.

In this paper the aim is to study the aqueous solution behavior of caffeic and *p*-coumaric acid in the presence of iron with cryo-transmission electron microscopy (cryo-TEM) and dynamic light scattering (DLS). The choice of including iron in this study is based on the fact that iron is commonly present in foods and is a common cause of oxidation. In numerous model studies of oxidation and antioxidant activity iron has also been added as a pro-oxidant.

MATERIALS AND METHODS

Caffeic acid and *p*-coumaric acid were purchased from Sigma (Sigma-Aldrich, St. Louis, MO), whereas iron(II)sulfate and imidazole

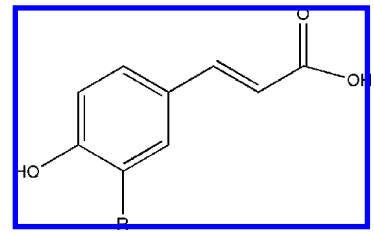

Figure 1. Chemical structure of the two phenolic acids investigated in this paper: *p*-coumaric acid (R = H) and caffeic acid (R = OH).

* Corresponding author (e-mail lars.nilsson@food.lth.se; telephone +46 46 2228303; fax +46 46 2224622).

† Division of Food Technology.

§ Division of Physical Chemistry 1.

Present address: R&D Wood Care and Paint, Dyrup A/S, Søborg, Denmark.

10.1021/jf8025925 CCC: $40.75
Published on Web 11/13/2008

were purchased from Merck (Darmstadt, Germany). The phenolic acids, caffeic and *p*-coumaric acid, were dissolved in pure water, and the pH was adjusted to 6.0. Iron(II)sulfate was dissolved in aqueous imidazole buffer solution (5 mmol/L, pH 6.0). All solutions were transparent and appeared as true solutions.

The precipitation was initiated by mixing appropriate amounts of each solution to obtain the desired concentration (0.6−2 mmol/L phenolic acid and 0.1−0.3 mmol/L Fe^{2+}). The tube was rapidly mixed and left to stand at room temperature for 24 h, after which a droplet was placed on a lacy carbon film supported by a copper grid and gently blotted with filter paper to obtain a thin liquid film. The grid was quenched in liquid ethane (−180 °C) and transferred to liquid nitrogen (−196 °C). The samples were transferred to the TEM (Philips CM120 BioTWIN Cryo) equipped with an energy filter imaging system (Gatan GIF 100) and an Oxford CT 3500 cryoholder and transfer system. The acceleration voltage was 120 kV and the working temperature, −180 °C.

The samples for the DLS experiments was prepared in the same manner as described above for the cryo-TEM experiments. The setup for the DLS measurements is an ALV/DLS/SLS-5000F, CGF-8F based compact goniometer system (ALV-GmbH, Langen, Germany). The light source is a CW diode-pumped Nd:YAG solid-state Compass-DPSS laser with a symmetrizer (Coherent, Santa Clara, CA). The laser operates at 532 nm with a fixed output power of 400 mW, varied using an attenuator from Newport Inc. The cylindrical glass cuvette is immersed into a cylindrical quartz container, containing refractive index matching liquid (decalin). The detection system includes a near monomodal optical fiber and two matched photomultipliers, put in a pseudocross geometry.

Analysis of the DLS data was performed by fitting the normalized experimentally measured time correlation function of the scattering intensity, $g^{(2)}(t)$. The model used in the fitting procedures is expressed with respect to the normalized time correlation function of the electric field, $g^{(1)}(t)$, which is related to $g^{(2)}(t)$ by Siegert's relationship

$$g^{(2)}(t) - 1 = \beta |g^{(1)}(t)|^2 \quad (1)$$

where t is the lag time and β is the coherence factor (≤ 1) that takes deviations from the ideal correlation and the experimental geometry into account. $g^{(1)}(t)$ can either be a single exponential function, with one corresponding relaxation time (t), or a multiexponential decay, depending on the system investigated. For a system that exhibits a distribution of relaxation times, $g^{(1)}(t)$ is described by a continuous function of the relaxation time using the Laplace transform

$$g^{(1)}(t) = \int_0^\infty A(\tau) \exp(-t/\tau)\, d\tau = \int_{-\infty}^{\infty} \tau A(\tau) \exp(-t/\tau)\, d \ln \tau \quad (2)$$

where $\tau = \Gamma^{-1}$ and Γ is the relaxation or frequency rate. By regularized inverse Laplace transformation (RILT), the relaxation time distribution $\tau A(\tau)$ can be obtained of the measured intensity correlation function $g^{(2)}(t)$. The REPES algorithm (incorporated in the GENDIST analysis package program) was used to analyze the data (*17*). In all analyses the "probability-to-reject term" was chosen to 0.5 as a standard. In this work we present the relaxation time distribution as $\tau A(\tau)$ versus log τ, which is also normalized with the maximum peak height. The translational diffusion coefficient, D, is related to the relaxation rate Γ, obtained in the RILT analysis, by

$$D = \lim_{q \to 0} \left(\frac{\Gamma}{q^2} \right) \quad (3)$$

where q is the absolute value of the scattering vector [$q = 4\pi n_0 \sin(\theta/2)/\lambda$, where n_0 is the refractive index of the solvent, λ is the incident wavelength, and θ is the scattering angle]. Knowing the translational diffusion coefficient D, the apparent hydrodynamic radius can be calculated by using the Stokes−Einstein equation (*18*)

$$R_{H,app} = \frac{kT}{6\pi\eta_0 D} \quad (4)$$

where k is the Boltzmann constant, T is the absolute temperature, and η_0 is the viscosity of the solvent

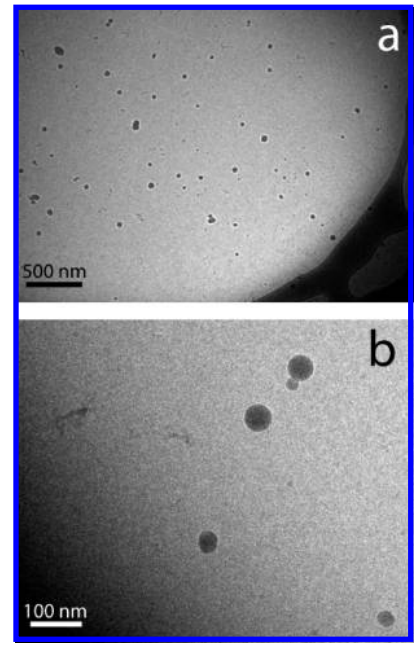

Figure 2. Cryo-TEM micrographs of iron−coumaric acid particles 24 h after the addition of iron to the coumaric acid solution. The iron and coumaric acid concentrations are 0.3 and 2 mmol/L, respectively.

RESULTS

Particles formed from solutions of iron (100−300 μmol/L) and caffeic or coumaric acid (600−2000 μmol/L) were studied with cryo-TEM and DLS. The results of the cryo-TEM experiments are shown as representative micrographs in **Figures 2** and **3**. From these figures it can be seen that the particles formed are in the nanometer range with diameters of approximately 20−50 nm for coumaric acid (**Figure 2**) and 10−150 nm for caffeic acid (**Figure 3**). Furthermore, the particles seem to be somewhat aggregated. This applies in particular for the iron−caffeic acid particles.

Figure 4 displays the size distribution for caffeic acid, 2 weeks after mixing. The distribution is obtained from an inverse Laplace transformation of the intensity correlation function from DLS measurements. The direct transformation from relaxation time distribution to size distribution is valid under the assumption that we are investigating small particles that do not possess any angular dependence and, hence, the contribution from the scattered light is related only to the translational diffusion processes of the particles. Measurements were also performed at additional angles, and the relaxation times were plotted as function of q^2, which is displayed in **Figure 5**. The figure shows a function that is perfectly linear and passes through the origin. This is an indication that the scattering contribution is purely related to the translational diffusion, which justifies our assumption previously discussed. The distribution peak in **Figure 4** is narrow, indicating rather monodisperse particles. $R_{H,app}$ of the particles is estimated to 20 nm. The transformation to $R_{H,app}$ is valid under the assumption that we are investigating small particles that scatter only once, so that the contribution is purely related to diffusion processes. The relaxation time distribution was gained from an inverse Laplace transformation of the autocorrelation function. Measurements were also performed earlier, immediately after mixing and 24 h after mixing. The sample measured immediately after mixing did not scatter and, thus, no particles were present. After 24 h, a peak in the same time regimen as in **Figure 4** was observed. However, this result has a large uncertainty as the intensity was low. The intensity increased 10 times between 24 h and 2 weeks. The results show

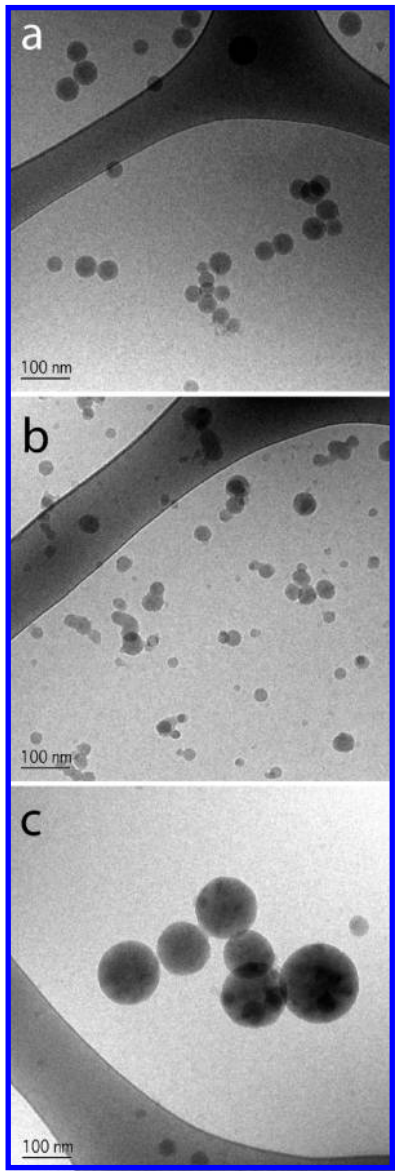

Figure 3. Cryo-TEM micrograph of iron−caffeic acid particles 24 h after the addition of iron to the caffeic acid solution. The iron and caffeic acid concentrations are 0.1 and 0.6 mmol/L, respectively (**a**), and 0.3 and 1.7 mmol/L, respectively (**b**, **c**).

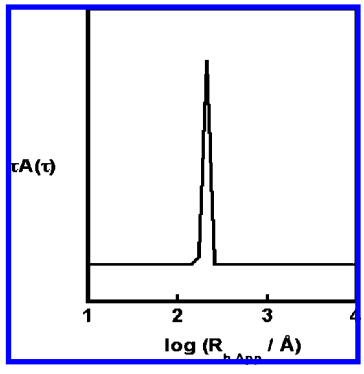

Figure 4. Relaxation rate (Γ) for the iron-caffeic acid mode as a function of the square of the magnitude of the scattering vector (q^2).

that the kinetics governing the formation of the particles is slow. Measurements were performed at additional angles, and the relaxation times were plotted as function of q^2. The function passed through the origin and showed perfect linear behavior,

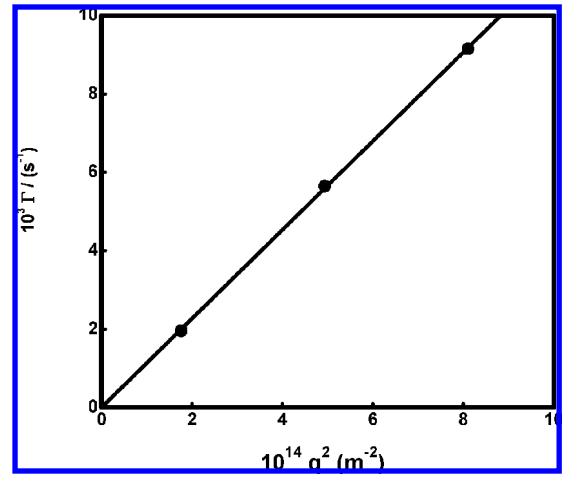

Figure 5. Size distribution recalculated from the relaxation time distribution obtained from inverse Laplace transformation of the intensity correlation function from DLS for iron-caffeic acid particles.

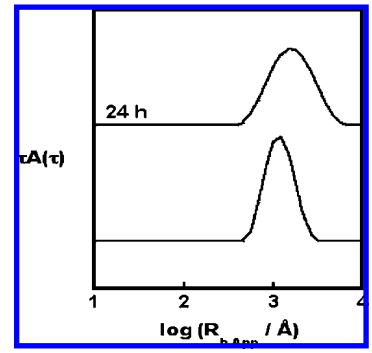

Figure 6. Size distributions recalculated from the relaxation time distributions obtained from inverse Laplace transformation of the intensity correlation function from DLS for iron-coumaric acid particles, directly after mixing (bottom) and 24 h after mixing (top).

which indicates that the modes are due to a translational diffusion process and also justify our assumption previously mentioned.

In **Figure 6** two size distribution functions are displayed. The bottom distribution function is attributed to a measurement performed directly after mixing, whereas the top function represents the same sample but 24 h after mixing. The distributions were obtained in the same way as described above for caffeic acid. **Figure 6** shows that, immediately after mixing, large particles are formed, which grow with time until they sediment. The hydrodynamic radius of the particles can be estimated to 100 nm immediately after mixing and 160 nm 24 h later. The intensity increased between the two measurements, and it can be seen that the distribution has shifted to the right, indicating an increase in size of the particles between the measurements. After 1 week, all of the particles were found as a sediment layer at the bottom of the measuring cell.

DISCUSSION

The results show that particles in the nanometer range are formed when iron, Fe^{2+}, in the range of 100−300 μmol/L is added to solutions of caffeic or coumaric acid. This is confirmed with both DLS and cryo-TEM. Furthermore, iron−caffeic acid particles appear to be rather monodisperse (**Figure 4**) and remain stable in size for at least 2 weeks. For these particles there is a good agreement between results obtained by DLS and those obtained from cryo-TEM. The particles consisting of iron−coumaric

acid have a wider distribution in sizes (**Figure 6**), which is less reflected in the cryo-TEM micrographs (**Figure 2**). Also, the estimated $R_{H,app}$ for iron−coumaric acid particles (**Figure 6**) is higher than radii observed in the cryo-TEM micrographs. This may be due to an overestimation of $R_{H,app}$ caused by the presence of low amounts of large particles.

An interesting aspect of the results is the rather large difference in behavior between the two phenolic acids. Caffeic acid seems to form meta-stable large particles, whereas the particles formed from *p*-coumaric acid grow more rapidly. Although the chemical structure of the two substances is quite similar, the interaction with iron is apparently different. The dissociation constants for the carboxyl group in the two substances are quite similar, 4.36−4.41 for caffeic acid (*19*−*21*) and 4.43 for coumaric acid (*21*), which is natural considering the similarity in chemical structure. It has been shown that the presence of the catechol moiety gives rise to a higher antioxidant activity in lipid systems (*22*) and, thus, caffeic acid is considered to be a more efficient antioxidant than *p*-coumaric acid. Furthermore, the catechol moiety also enhances the chelation of iron (*1*). From this it is, however, impossible to be conclusive on the difference in the results obtained for the two substances in the present paper.

The formation of metastable colloidal dispersions in the nanosize range makes observations regarding solubility very difficult. Thus, it is easy to understand that this phase separation previously has been overlooked and attracted only limited attention. However, when the possibility of equilibrium partitioning of phenolic acids between oil and water phases is discussed, this is, of course, essential.

Partitioning between water and oil phase has previously been proposed (*16*). This comes back to the issue of solubility. Partitioning between the phases can be described if an equilibrium can be defined where the activities in the respective phases are equal.

$$a_{\text{polyphenol/aq-phase}} = a_{\text{polyphenol/oil-phase}} \quad (5)$$

For a poorly soluble substance, such as a polyphenol in water or a polyphenol in oil, we may assume a Henry's law type behavior

$$a_{\text{polyphenol}} = \frac{c}{c^*} \quad (6)$$

where c is the solubility of the polyphenol and c^* is the solubility in equilibrium with the solid phase. The partitioning constant is defined as

$$k_{w/o} = \frac{c_{\text{polyphenol/aq-phase}}}{c_{\text{polyphenol/oil-phase}}} = \frac{c^*_{\text{polyphenol/aq-phase}}}{c^*_{\text{polyphenol/oil-phase}}} \quad (7)$$

where c is defined in the respective phase. If the concentration is below the solubility limit, the partitioning constant appears as a constant and equals the ratio between the solubility limits in respective phases according to eq 7.

However, if the present polyphenol concentration is above the solubility limit, the partitioning according to eq 7 is still valid, although only if the insoluble fraction is separated from the aqueous soluble and oil soluble fractions. If the insoluble material is present as macroscopic particles, this condition may appear obvious for an experimentalist. Furthermore, if the solid material appears as nanosized particles, as observed in this paper, they are difficult to observe as their contribution to the turbidity is small and no precipitate is visible. To separate the particles from an aqueous solution, extensive centrifugation is needed, and they are virtually impossible to separate from an emulsion system. On the basis of the results of this study as well as previous observations of precipitation in polyphenol systems (*23*), we may conclude that many determinations of partitioning constants may depend on the concentration applied and how the insoluble material is distributed.

The observed precipitation also has a critical influence on the mechanisms for the antioxidant activity. It seems clear that the formation of the precipitate should inhibit the pro-oxidant activity of the present iron. The observations in this study have been made using 100−300 μmol of Fe^{2+} equal to about 5−15 mg of Fe/L. These levels are high compared to typical impurity levels of ordinary foods but low compared to iron-containing foods. Most likely, the precipitation also indicates that chelating and complexation occur in solution also at concentration below which nanoparticles are formed. Thus, the observations in this study suggest that the complexing activity against common pro-oxidants is an important mechanism when antioxidant activity of phenolic acids is discussed.

A common feature in antioxidant studies is that the results vary, in an almost unpredictable manner, between studies. The experimental results in the current paper, showing slow precipitation kinetics, suggest a possible explanation for this variation.

LITERATURE CITED

(1) Andjelkovic, M.; Van Camp, J.; De Meulenaer, B.; Depaemelaere, G.; Socaciu, C.; Verloo, M.; Verhe, R. Iron-chelation properties of phenolic acids bearing catechol and galloyl groups. *Food Chem.* **2006**, *98* (1), 23–31.

(2) Sroka, Z.; Cisowski, W. Hydrogen peroxide scavenging, antioxidant and anti-radical activity of some phenolic acids. *Food Chem. Toxicol.* **2003**, *41* (6), 753–758.

(3) Foley, S.; Navaratnam, S.; McGarvey, D. J.; Land, E. J.; Truscott, T. G.; Rice-Evans, C. A. Singlet oxygen quenching and the redox properties of hydroxycinnamic acids. *Free Radical Biol. Med.* **1999**, *26* (9−10), 1202–1208.

(4) Caccetta, R. A. A.; Croft, K. D.; Beilin, L. J.; Puddey, I. B. Ingestion of red wine significantly increases plasma phenolic acid concentrations but does not acutely affect ex vivo lipoprotein oxidizability. *Am. J. Clin. Nutr.* **2000**, *71* (1), 67–74.

(5) Nardini, M.; Natella, F.; Scaccini, C.; Ghiselli, A. Phenolic acids from beer are absorbed and extensively metabolized in humans. *J. Nutr. Biochem.* **2006**, *17* (1), 14–22.

(6) DuPont, M. S.; Bennett, R. N.; Mellon, F. A.; Williamson, G. Polyphenols from alcoholic apple cider are absorbed, metabolized and excreted by humans. *J. Nutr.* **2002**, *132* (2), 172–175.

(7) Nardini, M.; Cirillo, E.; Natella, F.; Scaccini, C. Absorption of phenolic acids in humans after coffee consumption. *J. Agric. Food Chem.* **2002**, *50*, 5735–5741.

(8) Robaszkiewicz, A.; Balcerczyk, A.; Bartosz, G. Antioxidative and prooxidative effects of quercetin on A549 cells. *Cell Biol. Int.* **2007**, *31* (10), 1245–1250.

(9) Moltke Sörensen, A.-D.; Haahr, A.-M.; Miquel Becker, E.; Horsfelt Skibsted, L.; Bergenståhl, B.; Nilsson, L.; Jacobsen, C. Interactions between phenolic compounds, emulsifiers and pH in omega-3 enriched oil-in-water emulsions. *J. Agric. Food Chem.* **2008**, *56*, 1740–1750.

(10) RiceEvans, C. A.; Miller, N. J.; Paganga, G. Structure−antioxidant activity relationships of flavonoids and phenolic acids. *Free Radical Biol. Med.* **1996**, *20* (7), 933–956.

(11) Manach, C.; Williamson, G.; Morand, C.; Scalbert, A.; Remesy, C. Bioavailability and bioefficacy of polyphenols in humans. I. Review of 97 bioavailability studies. *Am. J. Clin. Nutr.* **2005**, *81* (1), 230S–242S.

(12) Chaiyasit, W.; Elias, R. J.; McClements, D. J.; Decker, E. A. Role of physical structures in bulk oils on lipid oxidation. *Crit. Rev. Food Sci. Nutr.* **2007**, *47* (3), 299–317.

(13) Silvestre, M. P. C.; Chaiyasit, W.; Brannan, R. G.; McClements, D. J.; Decker, E. A. Ability of surfactant headgroup size to alter lipid and antioxidant oxidation in oil-in-water emulsions. *J. Agric. Food Chem.* **2000**, *48*, 2057–2061.

(14) Donnelly, J. L.; Decker, E. A.; McClements, D. J. Iron-catalyzed oxidation of menhaden oil as affected by emulsifiers. *J. Food Sci.* **1998**, *63* (6), 997–1000.

(15) Porter, W. L. Paradoxical behavior of antioxidants in food and biological-systems. *Toxicol. Ind. Health* **1993**, *9* (1−2), 93–122.

(16) Schwarz, K.; Frankel, E. N.; German, J. B. Partition behaviour of antioxidative phenolic compounds in heterophasic systems. *Fett-Lipid* **1996**, *98* (3), 115–121.

(17) Schillen, K.; Brown, W.; Johnsen, R. M. Micellar sphere-to-rod transition in an aqueous triblock copolymer system—a dynamic light-scattering study of translational and rotational diffusion. *Macromolecules* **1994**, *27*, 4825–4832.

(18) Einstein, A. Uber die von der molekularkinatischen Theorie der Wärma geforderte Bewegung von in ruhenden Flussigkeiten suspendierten Teilchen. *Ann. Phys.* **1905**, *17*, 549–560.

(19) Silva, F. A. M.; Borges, F.; Guimaraes, C.; Lima, J.; Matos, C.; Reis, S. Phenolic acids and derivatives: studies on the relationship among structure, radical scavenging activity, and physicochemical parameters. *J. Agric. Food Chem.* **2000**, *48*, 2122–2126.

(20) Borges, F.; Lima, J.; Pinto, I.; Reis, S.; Siquet, C. Application of a potentiometric system with data-analysis computer programs to the quantification of metal-chelating activity of two natural antioxidants: caffeic acid and ferulic acid. *Helv. Chim. Acta* **2003**, *86* (9), 3081–3087.

(21) Sipila, J.; Nurmi, H.; Kaukonen, A. M.; Hirvonen, J.; Taskinen, J.; Yli-Kauhaluoma, J. A modification of the Hammett equation for predicting ionisation constants of *p*-vinyl phenols. *Eur. J. Pharm. Sci.* **2005**, *25* (4−5), 417–425.

(22) Chimi, H.; Cillard, J.; Cillard, P.; Rahmani, M. Peroxyl and hydroxyl radical scavenging activity of some natural phenolic antioxidants. *J. Am. Oil Chem. Soc.* **1991**, *68* (5), 307–312.

(23) Zanchi, D.; Vernhet, A.; Poncet-Legrand, C.; Cartalade, D.; Tribet, C.; Schweins, R.; Cabane, B. Colloidal dispersions of tannins in water−ethanol solutions. *Langmuir* **2007**, *23*, 9949–9959.

Received for review August 22, 2008. Revised manuscript received October 10, 2008. Accepted October 23, 2008. Financial support is gratefully acknowledged from the Program for New Antioxidant Strategies for Food Quality and Consumer Health (FOODANTIOX) supported by the Committee for Research and Development of the Öresund Region (Øforsk).

JF8025925